

1
2
3
4
5
6
7
8
9
10
11
12
13
14
15
16
17
18
19
20
21
22
23
24
25
26
27

DR. JINSHI JIAN (Orcid ID : 0000-0002-5272-5367)
DR. BEN BOND-LAMBERTY (Orcid ID : 0000-0001-9525-4633)
DR. DALEI HAO (Orcid ID : 0000-0001-7154-6332)
DR. JIANQIU ZHENG (Orcid ID : 0000-0002-1609-9004)
MS. KALYN DORHEIM (Orcid ID : 0000-0001-8093-8397)
MS. STEPHANIE PENNINGTON (Orcid ID : 0000-0003-2685-1092)
DR. WILLIAM R WIEDER (Orcid ID : 0000-0001-7116-1985)

Article type : Primary Research Article

Leveraging observed soil heterotrophic respiration fluxes as a novel constraint on global-scale models

Jinshi Jian^{1,2*}, Ben Bond-Lamberty², Dalei Hao³, Benjamin N. Sulman⁴, Kaizad F. Patel⁵, Jianqiu Zheng⁵, Kalyn Dorheim², Stephanie C. Pennington², Melannie D. Hartman^{6,7}, Dan Warner⁸, and William R Wieder^{7,9}

1. State Key Laboratory of Soil Erosion and Dryland Farming on the Loess Plateau, Northwest A&F University, Yangling, 712100, China
2. Pacific Northwest National Laboratory, Joint Global Change Research Institute at the University of Maryland–College Park, College Park, MD 20740, USA
3. Atmospheric Sciences and Global Change Division, Pacific Northwest National Laboratory, Richland, WA, USA
4. Climate Change Science Institute and Environmental Sciences Division, Oak Ridge National Laboratory, Oak Ridge, TN, US
5. Biological Sciences Division, Pacific Northwest National Laboratory, Richland, WA, USA

This is the author manuscript accepted for publication and has undergone full peer review but has not been through the copyediting, typesetting, pagination and proofreading process, which may lead to differences between this version and the [Version of Record](#). Please cite this article as [doi: 10.1111/GCB.15795](https://doi.org/10.1111/GCB.15795)

This article is protected by copyright. All rights reserved

- 28 6. Natural Resource Ecology Laboratory, Colorado State University, Fort Collins, CO, USA
- 29 7. Climate and Global Dynamics Laboratory, National Center for Atmospheric Research, Boulder,
30 CO 80307, USA
- 31 8. Delaware Geological Survey, University of Delaware, Newark, DE, USA
- 32 9. Institute of Arctic and Alpine Research, University of Colorado, Boulder, CO 80309, USA

33 * Corresponding author: Jinshi Jian

34 **Email:** jinshi@vt.edu

35 **ORCID:** 0000000252725367

36 **Keywords:** Soil organic carbon models, heterotrophic respiration, MIMICS, CASACNP, CORPSE,
37 benchmarking

38 **Running title:** Benchmarking biogeochemical models

39 **Abstract**

40 Microbially-explicit models may improve understanding and projections of carbon dynamics in response
41 to future climate change, but their fidelity in simulating global-scale soil heterotrophic respiration (R_H), a
42 stringent test for soil biogeochemical models, has never been evaluated. We used statistical global R_H
43 products, as well as 7,821 daily site-scale R_H measurements, to evaluate the spatio-temporal performance
44 of one first-order decay model (CASA-CNP) and two microbially-explicit biogeochemical models
45 (CORPSE and MIMICS) that were forced by two different input datasets. CORPSE and MIMICS did not
46 provide any measurable performance improvement; instead, the models were highly sensitive to the input
47 data used to drive them. Spatial variability in R_H fluxes was generally well simulated except in the
48 northern middle latitudes ($\sim 50^\circ\text{N}$) and arid regions; models captured the seasonal variability of R_H well,
49 but showed more divergence in tropic and arctic regions. Our results demonstrate that the next generation
50 of biogeochemical models shows promise, but also needs to be improved for realistic spatio-temporal
51 variability of R_H . Finally, we emphasize the importance of net primary production, soil moisture, and soil
52 temperature inputs, and that jointly evaluating soil models for their spatial (global scale) and temporal
53 (site scale) performance provides crucial benchmarks for improving biogeochemical models.

54 **1. Introduction**

55 The response of soil heterotrophic respiration (R_H) to environmental change will largely determine
56 whether soils are a carbon sink or source in the future (Bond-Lamberty *et al.*, 2018). Despite the critical
57 importance of microbes in driving this globally important carbon flux, current understanding of soil
58 microbial communities and their potential responses to climate change is highly uncertain (Crowther *et al.*,
59 2019). Most biogeochemical models use a first-order decay process to describe soil carbon decomposition
60 (Todd-Brown *et al.*, 2012), meaning that biological factors such as the size and composition of the
61 decomposer microbial community, interactions of organic matter with soil minerals and aggregates,
62 adaptations of microbial physiology, and priming are ignored (Schmidt *et al.*, 2011). This risks omitting
63 crucial climatic feedback as the Earth system transitions to a novel and uncertain future (Wieder *et al.*,
64 2015a).

65 New models seek to represent such potential biotic feedback to environmental change, but evaluation of
66 their carbon cycle representation and performance is nascent (Wieder *et al.*, 2015b). In recent years, many
67 efforts have been made to include microbial biogeochemical mechanisms into a new generation of
68 microbially-explicit models (Sulman *et al.*, 2014, 2018; Wieder *et al.*, 2014, 2015a, 2019). In theory,
69 these models offer considerable advantages over first-order decay approaches in projecting future climate
70 and carbon cycle feedback (e.g., they are capable of simulating population-driven dynamics independent
71 of abiotic drivers). However, uncertainties in process representation and parameterization have led to
72 divergent outcomes from different microbial-explicit models, leaving open questions of which if any
73 model formulations improve predictive accuracy (Sulman *et al.*, 2018).

74 Evaluating global-scale soil biogeochemical models is challenging, given the lack of appropriate datasets
75 that can serve as model benchmarks (Koven *et al.*, 2017; Collier *et al.*, 2018; Shi *et al.*, 2020). Wieder *et al.*
76 (2018, 2019) developed a biogeochemical testbed to compare the performance of a first-order model,
77 Carnegie-Ames-Stanford Approach (CASA-CNP) (Potter *et al.*, 1993; Randerson & Thompson, 1996;
78 Wang *et al.*, 2010) vs. two microbially-explicit models, including Microbial-MIneral Carbon Stabilization
79 (MIMICS) (Wieder *et al.*, 2014, 2015a), and Carbon, Organisms, Rhizosphere, and Protection in the Soil
80 Environment (CORPSE) (Sulman *et al.*, 2014, 2017). Such a testbed provides a consistent environment
81 for evaluating different models, similar to e.g. International Land Model Benchmarking (ILAMB)
82 (Collier *et al.*, 2018). This work showed that different models lead to divergent SOC predictions with a
83 distinct signature of heterotrophic respiration fluxes (Basile *et al.*, 2020; Wieder *et al.*, 2019).

84 Model performance needs to be evaluated by actual data. Wieder *et al.* (2013) and Wieder *et al.* (2015a)
85 compared carbon storage simulation from testbed models vs. Harmonized world soil database (HWSD)
86 carbon storage to evaluate the model performance. Basile *et al.* (2019) showed that spatial and temporal

87 variations in atmospheric CO₂ could be used to benchmark biogeochemical models. Predicting carbon
88 fluxes constitutes an equally and perhaps more stringent test for models, compared with projecting SOC
89 stocks or atmospheric CO₂ (Todd-Brown *et al.*, 2012, 2013). Heterotrophic respiration (R_H) is a direct
90 consequence of microbial activities, and therefore accurately simulating R_H is a key metric of model
91 performance, but R_H simulations from microbially-explicit models have never been compared with
92 observational benchmarks at global scale. Emerging global soil respiration (R_S) databases provide an
93 opportunity to evaluate models across different conditions based on *in situ* observations. Bond-Lamberty
94 *et al.* (2010) and Jian *et al.* (2020) compiled published annual R_S (which also includes estimates of annual
95 R_H) into a global R_S database (SRDB). Based on the SRDB, Jian *et al.* (2018) further compiled the daily
96 and monthly R_S (which also includes R_H measurements) into a global daily R_S database (DGRsD),
97 through which 7,821 daily R_H field measurements are available for model performance evaluation.
98 Meanwhile, new global R_H datasets have been developed (Hashimoto *et al.*, 2015; Warner *et al.*, 2019;
99 Tang *et al.*, 2020). Such field measurements and data-driven statistical R_H data products (Hashimoto *et al.*,
100 2015; Warner *et al.*, 2019; Tang *et al.*, 2020) offer promising opportunities to validate both existing first-
101 order and new microbially-explicit models' performance at site, regional, and global scales.

102 The objectives of this study are to: 1) evaluate differences between CASA-CNP, CORPSE, and MIMICS
103 models' predictions and observational benchmarks at multiple spatial scales; 2) investigate whether
104 microbially-explicit models (CORPSE and MIMICS) outperform the first-order model (CASA-CNP); and
105 3) explore the main reasons causing R_H mismatch between models and benchmarks. We analyzed R_H
106 simulations from CASA-CNP, CORPSE, and MIMICS with three global R_H data products derived from
107 statistical models and 7,821 daily site-scale R_H observations from DGRsD as benchmarks (Figure 1 and
108 Figure 2).

109 **2. Methods**

110 Previous studies have identified the importance of climate forcing in generating carbon cycle uncertainty
111 (Todd-Brown *et al.*, 2013). In this study, we further examine the role of climate forcing in generating R_H
112 uncertainty. The biogeochemical testbed is driven by external forcings that include gross primary
113 productivity, soil and air temperature, and soil moisture (Wieder *et al.*, 2018). We generated these inputs
114 from simulations with the Community Land Model, versions 4.5 (Oleson *et al.*, 2010) and 5.0 (Lawrence
115 *et al.*, 2019). The simulations were run in satellite phenology mode with the default climate reanalysis for
116 each model version: CLM4.5 uses atmospheric forcing data from National Centers for Environmental
117 Prediction and Climatic Research Unit (CLM4.5-CRUNCEP), and CLM5.0 uses the Global Soil Wetness
118 Project Phase 3 (CLM5.0-GSWP3). Although this approach complicates attributing differences in input

119 data to differences in model versions vs. climate forcings, previous work suggests that these combinations
120 provide the most realistic soil temperatures, especially at high latitudes (Bonan et al. 2019; Lawrence et al.
121 2019). This study used the forcing data from CLM as boundary conditions to drive the CASA vegetation
122 model, which generated net primary production (NPP) that was partitioned into different plant tissues and
123 litterfall that drive the accumulation and decomposition of soil C stock simulated by CASA-CNP,
124 MIMICS and CORPSE. We then compared the R_H fluxes simulated by the models to examine the R_H
125 simulation uncertainty related to different forcing data (Figure 2).

126 Heterotrophic respiration (R_H) data from a biogeochemical testbed, statistical global R_H datasets, as well
127 as daily timescale field R_H measurements were used in this study. For the biogeochemical testbed, the
128 CASA-CNP, CORPSE, and MIMICS models were driven by the inputs from the Community Land Model
129 (CLM, versions 4.5 and 5.0). These two versions of CLM were parameterized with different forcing
130 datasets: CLM4.5 uses atmospheric reanalysis from Climatic Research Unit of National Centers for
131 Environmental Prediction (CRUNCEP) for the period 1901-2010 (Wieder *et al.*, 2018); while CLM5.0
132 uses climate reanalysis from the Global Soil Wetness Project Phase 3 (GSWP3) for the period 1901-2014
133 (Dirmeyer *et al.*, 2006; Yoshimura & Kanamitsu, 2013). Daily modeled GPP, air and soil temperature,
134 and soil moisture were used to drive the CASA vegetation model, which generated NPP and partitioning
135 into different plant tissues and litterfall. Thus, the soil models experienced identical environmental drivers,
136 when forced by CLM4.5-CRUNCEP and CLM5.0-GSWP3 inputs, respectively. This experimental design
137 affords opportunities to evaluate uncertainties in external forcings (CLM4.5-CRUNCEP vs. CLM5.0-
138 GSWP3 forced simulations). It also allows us to isolate the effects of model structural uncertainty among
139 CASA-CNP, MIMICS, and CORPSE soil model formulations. This ensures that simulated R_H differences
140 from those three models are caused by the microbial processes (first-order decay vs. microbially-explicit)
141 and parametric differences between the models.

142 An exhaustive description of differences in the strengths and weaknesses of different versions of CLM is
143 outside the scope of this paper. Lawrence et al. (2019) documented significant improvements in CLM5.0,
144 relative to previous versions of the model. Notable improvements include reduced biases in gross primary
145 productivity (especially across mid- and high-latitude ecosystems), improved representation of permafrost
146 extent, and better agreement with observed terrestrial water storage anomalies. Similarly, Lawrence et al.
147 (2019) reported better agreement with model benchmarks for air temperature, precipitation, and solar
148 radiation for CLM simulations forced with GSWP3, compared to CRUNCEP forced runs. Thus, we
149 assumed the improvements from these data to the testbed models will carry forward to our R_H results.

150 The details regarding the microbial processes in CASA-CNP, CORPSE, and MIMICS can be found at
151 (Potter *et al.*, 1993; Randerson & Thompson, 1996; Wang *et al.*, 2010; Wieder *et al.*, 2013, 2014, 2015a,
152 2018; Sulman *et al.*, 2014, 2017), but we briefly described here: the CASA-CNP used first-order, linear
153 decay rates modified by soil temperature and soil moisture to simulate microbial R_H that are proportional
154 to soil organic matter pools (Potter *et al.*, 1993; Randerson & Thompson, 1996; Wang *et al.*, 2010);
155 MIMICS was designed to evaluate the interactions of microbial physiology and soil properties
156 (specifically soil texture) in moderating patterns of soil carbon persistence across large eco-climatological
157 gradients (Wieder *et al.*, 2014, 2015a). MIMICS uses a temperature-sensitive reverse Michaelis-Menten
158 kinetics to explicitly represent microbial activity that is moderated by substrate availability, soil
159 temperature, and the availability of liquid soil water (Wieder *et al.*, 2014, 2015b). MIMICS simulates the
160 activity of two microbial biomass communities that are characterized by having either rapid growth rate
161 and low growth efficiencies or slow growth rates and higher growth efficiencies. The turnover of these
162 microbial biomass pools are subject to density dependent microbial mortality rates as well as
163 environmental conditions. CORPSE was developed to examine the priming (increased carbon inputs due
164 to atmospheric CO_2 fertilization may accelerate old carbon decomposition) and protection (increased
165 carbon inputs are protected through interactions with mineral particles) responses of SOC to rising
166 atmospheric CO_2 (Sulman *et al.*, 2014). CORPSE also explicitly represents microbial activity and uses
167 modified Michaelis-Menten kinetics that are sensitive to substrate availability, soil temperature and liquid
168 water availability. CORPSE only represents a single microbial biomass pool and uses a fixed microbial
169 mortality rate (Sulman *et al.*, 2014, 2017; Georgiou *et al.*, 2017). In these simulations MIMICS and
170 CORPSE use the same function to modify soil C turnover based on liquid water availability (Sulman *et*
171 *al.*, 2014).

172 Global R_H data products were used to evaluate the performance of microbially-explicit models. There are
173 three global field-measurements-driven statistical R_H data products available, and all these R_H data
174 products were developed based on the same global R_S database (SRDB, version 3) (Bond-Lamberty &
175 Thomson, 2010) but used different modelling approaches. The first global R_H data product
176 (<http://cse.ffpri.affrc.go.jp/shojih/data/index.html>) was developed using a Metropolis–Hastings algorithm
177 to parameterize the relationship between R_S and climate factors (air temperature and precipitation) at the
178 site-level. Specifically, this algorithm was used to up-scale R_S from site to globe between 1965 and 2012
179 at $0.5^\circ \times 0.5^\circ$ spatial resolution (Hashimoto *et al.*, 2015). R_H was then calculated based on the
180 relationship between R_H and R_S [$\ln(R_H) = 1.22 + 0.73 \ln(R_S)$] from a global meta-analysis (Bond-
181 Lamberty *et al.*, 2004). As confidence interval (CI) of R_H was not directly reported, we calculated it
182 based on the CI of global soil respiration (R_S) and its CI based on Hashimoto *et al.* (2015), i.e., $CI(R_H) =$

183 $4 \times \frac{51}{91}$. The second R_H product (<https://doi.org/10.6084/m9.figshare.8882567>) was developed using a
184 random forest machine learning approach. Based on the third version of SRDB together with a R_H data
185 search, 504 annual R_H observations were used to train the relationship between R_H and 9 environmental
186 factors (including mean annual temperature, mean annual precipitation, diurnal temperature range,
187 nitrogen deposition, Palmer Drought Severity Index, shortwave radiation, soil carbon content, soil
188 nitrogen content, and soil water content) based on the random forest modelling approach. Then global
189 annual R_H and related CI between 1980 and 2016 were predicted at $0.5^\circ \times 0.5^\circ$ spatial resolution (Tang
190 *et al.*, 2020). The third global R_H data product
191 (https://daac.ornl.gov/CMS/guides/CMS_Global_Soil_Respiration.html) was developed using a quantile
192 regression forest modelling approach. Specifically, field data was used to train the relationship between
193 R_S and four environmental factors (mean annual temperature, mean annual precipitation, enhanced
194 vegetation index, and mean winter precipitation) (Warner *et al.*, 2019), and mean annual R_H was then
195 predicted at 1 km spatial resolution based on the R_H and R_S relationship [$\ln(R_H) = 1.22 + 0.73 \ln(R_S)$].
196 Warner *et al.* (2019) did not report CI, so we first calculated CI of R_S pixels (generated as CI of the mean
197 of all random forest "trees" predictions at each pixel, was 4.7 Pg), and then calculated $\text{CI}(R_H) = 4.7 \times$
198 $\frac{49.8}{87.9}$.

199 Daily R_H measurements at the site scale were collected to evaluate the seasonal performance of
200 microbially-explicit models at finer time and spatial scales. We went through the studies in SRDB which
201 reported annual R_H measurements (red crosses in Figure 1), and checked whether detailed daily R_H
202 measurements were reported; we then compiled these daily R_H measurements into DGRsD. In total 7,821
203 daily R_H observations from 254 studies were obtained (Figure 1, blue circles). We used latitude, longitude,
204 year, and day of year to link these DGRsD data with the models' R_H outputs and thus obtain modeled R_H
205 for all the observational sites and sampling times. Note that the spatial resolution of CASA-CNP,
206 CORPSE, and MIMICS is 2.0° latitude \times 2.5° longitude, meaning an inevitable spatial mismatch as we
207 thus compare site-specific observations with grid cell-scale model outputs (Shao *et al.*, 2013). In addition,
208 the CASA-CNP, CORPSE, and MIMICS runs ended in 2010 and 2014 (for CLM4.5-CRUNCEP and
209 CLM5.0-GSWP3 forced simulations, respectively) but observational data for some sites were as late as
210 2017. In these cases, we used the 2000-2010 (when driven by CLM4.5-CRUNCEP) and 2000-2014
211 (when driven by CLM5.0-GSWP3) model average of a 3-day window around the observational date; for
212 example, an R_H value measured on June-20th 2015 would be linked with the modeled R_H between June-
213 17th and June-23th, averaged over the 2000-2010 period (CLM4.5-CRUNCEP forcing) or 2000-2014
214 period (CLM5.0-GSWP3 forcing). We did this because our focus was not on evaluating model
215 performance at the daily scale, but rather the correctness of its overall seasonality. We then calculated

216 mean R_H (measured R_H as well as predicted R_H by CASACNP, MIMICS, and CORPSE) and their
217 confidence interval (CI, within a specific group, $CI = t_{score} \times \text{standard error}$) by day of year within six
218 climate regions (Tropic, Arid, Temperate, Mediterranean, Boreal, and Arctic) to analyze models also
219 reasonably capture the seasonal pattern of R_H in different climates.

220 Global scale R_H fluxes between 1980 and 2010 for CLM4.5-CRUNCEP, between 1980 and 2014 for
221 CLM5.0-GSWP3 from the biogeochemical models (CASA-CNP, CORPSE, and MIMICS models) were
222 compared with that from the global R_H statistical products as well as daily R_H measurements collected
223 from 254 studies (Figure 1). Specifically, we investigated whether biogeochemical models can predict the
224 magnitude and trend of global annual R_H under global climate change (Figure 2). Global annual R_H were
225 summed up based on R_H rate and the area of each cell. We calculated global annual R_H between 1980 and
226 2016 when possible. We then compared R_H latitudinal patterns from the biogeochemical models vs. that
227 from the global R_H data to investigate whether biogeochemical models well capture the R_H spatial
228 variability. The spatial resolution of biogeochemical models and the global R_H data varied from 0.5 to
229 2.5 °, therefore, we averaged R_H rate by every 5 ° along the latitude gradient. Mean R_H rates along each
230 latitude were then compared. We also compared NPP outputs from the CASA-CNP model vs. MODIS
231 NPP (<https://code.earthengine.google.com/>) (Zhao *et al.*, 2005) to evaluate whether the difference
232 between modeled R_H and benchmark R_H is related to the NPP inputs bias.

233 Site scale daily R_H vs. the prediction from the biogeochemical models was compared to investigate
234 whether microbially-explicit models well predict daily and site scale R_H . Based on the latitude, longitude,
235 and time information, we retrieved the R_H predictions from the three biogeochemical models. Linear
236 regression was used to analyze the linear relationship between measured R_H and model predicted R_H . The
237 raw data do not follow a normal distribution and thus it is difficult to compare the difference between
238 measured R_H and modeled R_H . We thus used a bootstrap resampling approach to sample the mean of R_H
239 from both measured and modeled R_H 10,000 times, and a non-parametric Wilcoxon test was then used to
240 test whether modeled R_H were different from the measured R_H .

241 We further used the Wilcoxon test to compare the modeled R_H vs. measured R_H . From DGRsD, there are
242 254 studies with more than 5 R_H observations, for each study, we applied a non-parametric Wilcoxon test
243 to investigate whether modeled R_H significantly differs from measured R_H . Based on the Wilcoxon-test p
244 value and mean error (ME, i.e., mean of modeled R_H - measured R_H in each study, equation 1), all sites
245 could be separated into three groups: overestimated ($p \leq 0.05$ and $ME > 0$), underestimated ($p \leq 0.05$ and
246 $ME < 0$), and well estimated ($p \geq 0.05$).

247
$$ME = \frac{\sum_{i=1}^n (\hat{y}_i - y_i)}{n} \quad [1]$$

248 where \hat{y}_i represents the i_{th} predicted R_H value and y_i represents the i_{th} measured R_H value (Yang *et al.*,
249 2014).

250 To investigate whether the R_H differences between models and benchmarks are related with model NPP
251 inputs, we collected the MODIS NPP data from 2000-2019 using the platform of Google Earth Engine
252 (<https://code.earthengine.google.com/>). Specifically, we used the MOD17A2H V6 NPP product, which
253 has a 8-day temporal resolution and 500m spatial resolution (Zhao *et al.*, 2005). We further calculated the
254 annual mean value and latitude gradient of MODIS NPP. We collected the NEE data covering 2001-2015
255 from the FLUXCOM project, which aims to upscale biosphere-atmosphere fluxes from local FLUXNET
256 sites to continental and global scales (Tramontana *et al.*, 2016; Jung *et al.*, 2019). Here we used the
257 monthly 0.5° latitude \times 0.5° longitude FLUXCOM data with the setup of remote sensing to derive the
258 annual mean values of NEE globally.

259 3. Results

260 Global annual R_H from CASA-CNP, CORPSE, and MIMICS driven by CLM4.5-CRUNCEP (51.0 Pg C
261 yr^{-1} , all annual R_H from three models averaged, Figure 3a) forcing is in the range of that from statistical
262 models (47.2 - 58.9 Pg C yr^{-1} , Figure 3a) (Hashimoto *et al.*, 2015; Warner *et al.*, 2019; Tang *et al.*, 2020).
263 Latitudinally, R_H from CASA-CNP, CORPSE, and MIMICS match well with R_H from the statistical
264 models, but exhibited a mismatch in the northern mid-latitudes and arid regions (Figure 3b). However,
265 global annual R_H from CASA-CNP, CORPSE, and MIMICS driven by CLM5.0-GSWP3 (43 Pg C yr^{-1} ,
266 all annual R_H from three models averaged, Figure 3a) forcing is lower than that from statistical models
267 (47.2 - 58.9 Pg C yr^{-1}). Differences in the global sum of R_H fluxes (Figure 3a) reflect higher net primary
268 productivity with the CLM4.5 CRU-NCEP forced simulations, relative to the CLM5.0-GSWP3 forced
269 simulations (Figure 3c). The spatial distribution of the fluxes, however, suggest that CRU-NCEP forced
270 simulations have larger C fluxes in mid- to high latitudes (centered around 50 degrees N), which do not
271 agree with upscaled R_H observations (Figure 3b and Figure 4).

272 In the site-scale comparison, when driven by CLM4.5-CRUNCEP, we found that for most of the sites,
273 model-simulated R_H is higher than the field measured R_H (Figure 4). A non-parametric Wilcoxon test
274 shows that within 254 studies we investigated, CASA-CNP, CORPSE, and MIMICS driven by CLM4.5-
275 CRUNCEP overestimated R_H for 169 sites (66%), underestimated R_H for 65 sites (26%), and only
276 simulated R_H well for 8% of sites (Figure 4b). When driven by CLM5.0-GSWP3 forcing, the model

277 performance improved, as Root Mean Square Error (RMSE) decreased when compared with the results
278 driven by CRUNCEP (Figure S4). In addition, CASA-CNP, CORPSE, and MIMICS overestimated R_H
279 for 128 sites (50%), underestimated R_H for 96 sites (38%), and simulated R_H well for the remaining 30
280 (12%) sites (Figure 4e). The spatial pattern of R_H differences between CASA-CNP (averaged between
281 2000 and 2010) and Warner *et al.* (2019) showed that CASA-CNP overestimated R_H in northern middle
282 latitudes (Figure 4a). This problem was largely resolved when using GSWP3 to drive the model runs
283 (Figure 4d), however, model predicted R_H were still slightly higher than the measured R_H (Figure 5). The
284 spatial patterns of R_H from Hashimoto *et al.* (2015) and Tang *et al.* (2020) were almost identical to
285 Warner *et al.* (2019) (Figure S1). A similar conclusion could be obtained by comparing the distribution of
286 R_H simulations of CASA-CNP, CORPSE, and MIMICS with daily time scale R_H measurements from
287 individual sites (Figure 5).

288 When simulated R_H were compared with measured R_H by month and climate region, we found large
289 disagreements in most months and climate regions (Figure S2). A linear regression analysis ($n=7,821$)
290 showed that R_H simulations from MIMICS driven by CLM5.0-GSWP3 were weakly correlated with the
291 field observations ($R^2 = 0.11$); comparable percentages of variance explained for CASA-CNP and
292 CORPSE were 10.0% and 4.0%, respectively (Figure S3). The low correlation between field R_H
293 measurements and modeled R_H may result from the coarse spatial resolution of the testbed results ($\sim 2.0^\circ$
294 latitude \times 2.5° longitude), and they are compared to site-level (typically 0.1-1.0 km²) measurements.

295 The process models reasonably capture the seasonal pattern of R_H (Figure S5), but show differences when
296 separated into six climate regions, all models performance well in temperate ($R^2 > 0.40$) and boreal ($R^2 >$
297 0.50), but not for other climate regions ($R^2 < 0.20$, Figure 6). The seasonal pattern of modeled R_H was
298 also improved when driven by CLM5.0-GSWP3, especially in tropic and boreal regions (Figure 6). In
299 general, MIMICS captures the R_H seasonal variability slightly better compared with CORPSE, but similar
300 as CASA-CNP (Figure 6). However, MIMICS simulated R_H seems to have a later peak in the fall,
301 inconsistent with observations (Figure 6), a finding consistent with Basile *et al.* (2020). In the tropics, the
302 process models were unable to capture the large temporal amplitude of R_H (Figure 6). Similarly, in the
303 arctic, measured R_H showed a clear peak in the growing season, but models fail to capture this pattern.

304 4. Discussion

305 Biases in simulated R_H fluxes are strongly influenced by potential biases in plant productivity simulated
306 in the testbed models. The spatial distribution of R_H differences (biases, calculated as CASA-CNP
307 modeled R_H - observed R_H) showed a similar spatial pattern as the differences between CASA-CNP
308 modeled NPP and Moderate Resolution Imaging Spectroradiometer (MODIS) NPP (NPP differences,

309 Figure 4c and 4f). Specifically, large positive biases in simulated R_H fluxes from the CLM4.5-CRUNCEP
310 forced simulations occurred in mid latitudes ($\sim 50^\circ$ N) where we also found positive biases in simulated
311 NPP, compared with MODIS estimates. These productivity biases were reduced in the CLM5.0-GSWP3
312 forced simulations, leading to an improvement in simulated R_H as well.

313 However, NPP inputs alone cannot explain the process models' overestimation of R_H . For example,
314 underestimated R_H were mostly observed at central Australia and Tibet Plateau (Figure 4a, 4b, and Figure
315 S1a), but CASA-CNP modeled NPP showed no differences compared with the MODIS NPP there (Figure
316 3c, Figure 4c and 4f). One possibility is that the autotrophic and heterotrophic carbon fluxes simulated by
317 the land models will largely balance out, but observationally derived data products of NPP and R_H are not
318 necessarily internally consistent with each other. Indeed, the Net Ecosystem Exchange (NEE) that would
319 be derived from the difference between observationally based NPP and R_H estimates would produce large
320 carbon sinks across the tropics and middle latitudes according to the FLUXCOM NEE products
321 (Tramontana *et al.*, 2016; Jung *et al.*, 2019), but this carbon sink is poorly captured by these simulations
322 (Figure 3d).

323 When using GSWP3 as model forcing, the site scale daily R_H comparison showed that simulated R_H from
324 CASA-CNP, CORPSE, and MIMICS are much closer to the measured R_H , while annual R_H from model
325 results from CLM5.0-GSWP3 forcing (43 Pg C yr^{-1} , Figure 3a) are lower than the statistical benchmarks
326 ($47.2 - 58.9 \text{ Pg C yr}^{-1}$) (Hashimoto *et al.*, 2015; Warner *et al.*, 2019; Tang *et al.*, 2020). What might cause
327 these discrepancies? First, we recognize that gridded statistical estimates of R_H fluxes are themselves
328 uncertain. For example, lower global R_H has been reported by calculating R_H from satellite-driven
329 estimates (global $R_H = 43.6 \pm 19.3 \text{ Pg C yr}^{-1}$; mean \pm SD) (Konings *et al.*, 2019) and by a comprehensive
330 global bottom-up carbon budget accounting (global $R_H = 39 \pm 6 \text{ Pg C yr}^{-1}$) (Ciais *et al.*, 2020) compared
331 with the estimates from statistical models shown in Figure 3 (Hashimoto *et al.*, 2015; Warner *et al.*, 2019;
332 Tang *et al.*, 2020). Second, Jian *et al.*, (2018a) suggests that R_S sites' uneven distribution from the global
333 R_S database causes about 6 Pg C overestimate of global annual R_S . Finally, Jian *et al.*, (2018b) also
334 posited that the temporal variability of soil respiration plays an important role on global soil respiration
335 modeling and estimates, with global soil respiration prediction based on monthly soil respiration data
336 about 10 Pg C smaller than that based on annual data. This suggests that the mismatch between modeled
337 R_H (driven by GSWP3 forcing) and benchmarks may be related to R_S sites spatial uneven distribution and
338 temporal variability in R_H fluxes.

339 Another potential source of bias in the models, compared to observationally extrapolated R_H fluxes, is that
340 the modeled ratio of R_H to NPP in the biogeochemical models is too high. The value of R_H to NPP ratio

341 reported by the IPCC assessment report is 0.9 (Stocker *et al.*, 2013), and in testbed models this ratio is
342 almost 1 (i.e., NEE values are very close to 0, Figure 3d). R_H to NPP ratio estimates from IPCC and
343 testbed models, however, may be too high because the models generally do not consider dissolved and
344 particulate organic carbon losses to rivers and erosion (Cole *et al.*, 2007; Tan *et al.*, 2020), crop harvest
345 and grazing (Guenther *et al.*, 2012; Ciais *et al.*, 2020), or carbon emission due to fire (Werf *et al.*, 2017).
346 As a result, Tan *et al.* (Tan *et al.*, 2020) suggested that too much carbon is transferred to soils in the
347 models compared to reality, which results in a higher R_H to NPP ratios. This suggests that the associated
348 turnover time (and thus CO_2 emissions) of soil C pools may be more uncertain than currently thought
349 (Carvalhais *et al.*, 2014).

350 Alternatively, higher R_H estimates from biogeochemical models could be due to model parameterizations
351 with too-low carbon use efficiency (relative to transfers among soil C pools) (Geyer *et al.*, 2016).
352 Microbially-explicit models advance the representation of SOC dynamics and turnover under global
353 climate change, but parameterizing them remains an outstanding challenge (Wieder *et al.*, 2015b, 2018;
354 Bradford *et al.*, 2016). The field observations compiled in this study can be used to constrain the model
355 parameters for the next generation model improvement. Similarly, Zhang *et al.* (2020) used data from 72
356 sites in Europe and 134 sites in China to calibrate the parameter for SOC deprotection rate, improving the
357 performance of MIMICS. The key parameters related to SOC decomposition in the default CORPSE and
358 MIMICS (such as the microbial temperature sensitivity and microbial mortality rate) were parameterized
359 using laboratory (German *et al.*, 2012) and field data (Wieder *et al.*, 2013, 2014, 2015b), but increasing
360 field data collected from different environments across the globe should improve these models’
361 performance. This also emphasizes the need to collect relevant environmental covariates, especially soil
362 temperature and soil moisture data, as well as site level data on plant productivity and soil characteristics
363 from field R_S studies.

364 Such model benchmarking, evaluation, and diagnosis exercises are most powerful—provide the most
365 scientific benefit—when performed using high spatio-temporal resolution global R_H data products (Collier
366 *et al.*, 2018). Currently, there are three global observation-driven statistical R_H data products available,
367 but each was developed from the same underlying global R_S database (SRDB, version 3) (Bond-Lamberty
368 & Thomson, 2010), reducing their independence and thus benefit for benchmarking. In addition, currently
369 global R_H estimates are available only on annual timescales. Nonetheless, incorporating these
370 observations into benchmarking packages such as ILAMB (Collier *et al.*, 2018) will provide useful tests
371 to evaluate the representation of soil biogeochemistry in land models. Higher frequency daily and
372 monthly R_H fluxes are likely necessary to understand and evaluate the different sensitivities in soil
373 biogeochemical models, sub-annual biases and transient processes that produce hot spots and hot

374 moments (Bernhardt *et al.*, 2017), and the distribution and occurrence of extreme values across temporal
375 and spatial scales.

376 **Conclusion**

377 Microbially-based soil models likely hold the key to predicting 21st-century soil carbon climate feedback
378 accurately, but their development and evaluation remains a challenge. This study is the first to evaluate
379 such models' heterotrophic respiration fluxes against observed R_H at both local and global scales. The
380 three biogeochemical models we evaluated (the first-order land model CASA-CNP, and the microbial
381 CORPSE and MIMICS models) reasonably simulate annual R_H and its spatio-temporal variability
382 compared to three data-driven statistical global R_H data products and site-scale daily measurements. The
383 forcing dataset CLM5.0-GSWP3 provided significantly improved results compared to CLM4.5-
384 CRUNCEP. The spatial variability of R_H from the biogeochemical models is highly affected by the model
385 NPP and litterfall inputs, and all models exhibited temporal biases at the site scale. We conclude that (i) it
386 is important to improve NPP and litterfall (i.e., the carbon inputs to soil heterotrophs) in the next
387 generation of biogeochemical models; (ii) joint evaluations of models at multiple spatial and temporal
388 scales provides a stringent test of their performance; and (iii) microbial models' performance, at least in
389 the group examined here, is already at least as good as traditional first-order alternatives, high temporal-
390 and spatial-resolution datasets will be key to evaluating and improving these models in the future.

391 **Acknowledgments:** J.J was supported by the Strategic Priority Research Program of Chinese
392 Academy of Sciences (No. XDA20040202). B.B.-L., B.N.S., K.F.P, J. Z., K. D., S.C.P, and J.J were
393 supported by the US Department of Energy, Office of Science, Biological and Environmental Research as
394 part of the Terrestrial Ecosystem Sciences Program. The Pacific Northwest National Laboratory is
395 operated for DOE by Battelle Memorial Institute under contract DE-AC05-76RL01830. W.R.W. was
396 supported by the U.S. Department of Energy under award number BSS DE-SC0016364, US Department
397 of Agriculture NIFA Award number 2015-67003-23485, and NASA NNX17AK19G. D.H. was supported
398 by the U.S. National Oceanic and Atmospheric Administration (NOAA) under award number NOAA-
399 OAR-CPO-2019-2005530.

400 **Data and materials availability:** All code used in this analysis are available at
401 <https://github.com/PNNL-TES/landmodels>. Data outputs from CASA-CNP, CORPSE, and MIMICS are
402 too big to share at GitHub, please contact the corresponding author if users are interested in using the data
403 to reproduce all the results.

404 **Author Contributions:** W.R.W., B.B.-L., and J.J. conceived this study and designed the primary analysis.
405 W.R.W., M.D.H. and B.N.S. prepared heterotrophic respiration outputs from CASA-CNP, CORPSE, and
406 MIMICS driven by CLM4.5-CRUNCEP as well as CLM5.0-GSWP3. D.H., K.D., and S.P processed and
407 analyzed the spatial distribution of heterotrophic respiration data. J.J. and W.R.W. wrote the manuscript
408 in close collaboration with all authors. All authors provided feedback and insights in all phases.

409 **Competing Interest Statement:** None.

410 **Figure caption**

411 **Figure 1.** Geographic distribution of heterotrophic respiration (R_H) sites from the daily global soil
412 respiration (R_S) database (DGRsD, daily R_H collected from 254 individual articles, show as blue circles)
413 (Jian *et al.*, 2018) and a global R_S database (SRDB, red crosses) (Bond-Lamberty & Thomson, 2010);
414 Three global R_H datasets (Hashimoto *et al.*, 2015; Warner *et al.*, 2019; Tang *et al.*, 2020) were developed
415 based on annual R_S or R_H measurements. Point sizes represent the number of observations in each
416 location (unique latitude and longitude).

417

418 **Figure 2.** Diagram shows the workflow of this study. Data driven statistical global R_H products
419 (Hashimoto *et al.*, 2015; Warner *et al.*, 2019; Tang *et al.*, 2020) and filed R_H measurements collected
420 from articles were used as the benchmarks for the biogeochemical models (CASA-CNP, CORPSE, and
421 MIMICS) in this study. We compared the spatio-temporal variability of R_H to evaluate the performance of
422 biogeochemical models. Net Primary Production (NPP) and Net Primary Exchange (NEE) from
423 Moderate Resolution Imaging Spectroradiometer (MODIS) (Zhao *et al.*, 2005) and FLUXCOM
424 (Tramontana *et al.*, 2016; Jung *et al.*, 2019) are used to investigate whether the R_H differences between
425 models and benchmarks are related with model NPP inputs.

426

427 **Figure 3. (a)** Comparison of global annual mean heterotrophic respiration (R_H) predicted by data driven
428 statistical models (benchmark) (Hashimoto *et al.*, 2015; Warner *et al.*, 2019; Tang *et al.*, 2020) and
429 biogeochemical models (CASA, CORPSE, and MIMICS forced by CLM4.5-CRUNCEP and CLM5.0-
430 GSWP3). The shaded area showed the confidence interval (CI) of R_H . **(b)** Zonal mean R_H (mean rate: g C
431 $\text{m}^{-2} \text{yr}^{-1}$) along latitude, R_H predicted by Warner *et al.*, (2019) is used as a benchmark, R_H simulated by
432 CASA-CNP using CLM4.5-CRUNCEP and CLM5.0-GSWP3 forcings are compared with the benchmark
433 (within a specific zonal band, e.g., $85^\circ - 90^\circ$, CI of (Warner *et al.*, 2019) was calculated according to $\text{CI} =$
434 $t_{\text{score}} \times \text{standard error}$, CI of NPP and NEE benchmarks were calculated similarly); **(c)** Zonal mean Net
435 Primary Production (NPP) fluxes with latitude (mean rate between 1980 and 2010: $\text{g C m}^{-2} \text{yr}^{-1}$), NPP
436 (with CI) from MODIS is showed as the benchmark. **(d)** Zonal mean Net Ecosystem Exchange (NEE)
437 with latitude (mean rate between 1980 and 2010: $\text{g C m}^{-2} \text{yr}^{-1}$, $\text{NEE} = R_H - \text{NPP}$ for simulations), NEE
438 (with CI) from FLUXCOM (Tramontana *et al.*, 2016; Jung *et al.*, 2019) is showed as the benchmark.
439 Note that CI of MODIS NPP and FLUXCOM NEE are also shown in panel c and d, but they are too
440 small to see clearly.

441
442 **Figure 4.** (a) Global spatial distribution of soil heterotrophic respiration (R_H) differences between CASA-
443 CNP (driven by CLM4.5-CRUNCEP forcing) and data-driven statistical model result from ref (Warner *et*
444 *al.*, 2019); (b) R_H differences between CASA-CNP (driven by CLM4.5-CRUNCEP forcing) and daily
445 measured R_H from 254 studies. (c) NPP differences between CASA-CNP model and MODIS data. (d, e,
446 and f) similar as a, b, and c, but CASA-CNP was driven by CLM5.0-GSWP3 forcing.

447
448 **Figure 5.** Distributions of bootstrap resampled measured daily R_H and daily R_H predicted from CASA-
449 CNP, CORPSE, and MIMICS models driven by CLM4.5-CRUNCEP forcing and CLM5.0-GSWP3
450 forcing.

451
452 **Figure 6.** Heterotrophic respiration (R_H) seasonal pattern (averaged by day of year) across tropic, arid,
453 temperate, mediterranean, boreal, and arctic. Panels from left to right are the comparison between
454 measured R_H (gray) and CASA modeled R_H driven with CRUNCEP forcing, CASA modeled R_H driven
455 with GSWP3 forcing, CORPSE modeled R_H driven with GSWP3 forcing, and MIMICS modeled R_H
456 driven with GSWP3 forcing. The temporal trend of R_H simulated by CORPSE and MIMICS driven by
457 CRUNCEP forcing were almost identical to R_H simulated driven by GSWP3, therefore the results were
458 not shown. Note that only measurements from the northern hemisphere were used. R^2 and RMSE are
459 from the linear regression between measured R_H and model predicted R_H .

460

461 **References**

- 462 Basile, S.J., Lin, X., Wieder, W.R., Hartman, M.D. & Keppel-Aleks, G. (2020) Leveraging the signature
463 of heterotrophic respiration on atmospheric CO₂ for model benchmarking. *Biogeosciences*, 17(5):
464 1293-1308. <https://doi.org/10.5194/bg-17-1293-2020>.
- 465 Bernhardt E. S., Blaszczyk J. R., Ficken C. D., Fork M. L., Kaiser K. E. & Seybold E. C. (2017). Control
466 Points in Ecosystems: Moving Beyond the Hot Spot Hot Moment Concept. *Ecosystems* , 20(4), 665–
467 682. <https://doi.org/10.1007/s10021-016-0103-y>.
- 468 Bonan, G. B., Lombardozzi, D. L., Wieder, W. R., Oleson, K. W., Lawrence, D. M., Hoffman, F. M., &
469 Collier, N. (2019). Model Structure and Climate Data Uncertainty in Historical Simulations of the
470 Terrestrial Carbon Cycle (1850–2014). *Global Biogeochemical Cycles*, 33(10), 1310-1326. doi:
471 10.1029/2019gb006175.
- 472 Bond-Lamberty B., Wang C. & Gower S. T. (2004). A global relationship between the heterotrophic and
473 autotrophic components of soil respiration? *Global change biology*, 10(10), 1756–1766.
474 <https://doi.org/10.1111/j.1365-2486.2004.00816.x>.
- 475 Bond-Lamberty B. & Thomson A. (2010). A global database of soil respiration data. *Biogeosciences* ,
476 7(6), 1915–1926. <https://doi.org/10.5194/bg-7-1915-2010>.
- 477 Bond-Lamberty B., Bailey V. L., Chen M., Gough C. M. & Vargas R. (2018). Globally rising soil
478 heterotrophic respiration over recent decades. *Nature*, 560(7716), 80–83.
479 <https://doi.org/10.1038/s41586-018-0358-x>.
- 480 Bradford M. A., Wieder W. R., Bonan G. B., Fierer N., Raymond P. A. & Crowther T. W. (2016).
481 Managing uncertainty in soil carbon feedbacks to climate change. *Nature climate change*, 6(8), 751–
482 758. <https://doi.org/10.1038/nclimate3071>.
- 483 Carvalhais N., Forkel M., Khomik M., Bellarby J., Jung M., Migliavacca M., ... Reichstein M. (2014).
484 Global covariation of carbon turnover times with climate in terrestrial ecosystems. *Nature*,
485 514(7521), 213–217. <https://doi.org/10.1038/nature13731>.
- 486 Ciais P., Yao Y., Gasser T., Baccini A., Wang Y., Lauerwald R., ... Zhu D. (2020). Empirical estimates
487 of regional carbon budgets imply reduced global soil heterotrophic respiration. *National Science*
488 *Review*. <https://doi.org/10.1093/nsr/nwaa145>.
- 489 Cole J. J., Prairie Y. T., Caraco N. F., McDowell W. H., Tranvik L. J., Striegl R. G., ... Melack J. (2007).
490 Plumbing the Global Carbon Cycle: Integrating Inland Waters into the Terrestrial Carbon Budget.
491 *Ecosystems* , 10(1), 172–185. <https://doi.org/10.1007/s10021-006-9013-8>.

- 492 Collier N., Hoffman F. M., Lawrence D. M., Keppel-Aleks G., Koven C. D., Riley W. J., ... Randerson J.
493 T. (2018). The International Land Model Benchmarking (ILAMB) System: Design, Theory, and
494 Implementation. *Journal of Advances in Modeling Earth Systems*, 10(11), 2731–2754.
495 <https://doi.org/10.1029/2018MS001354>.
- 496 Crowther T. W., van den Hoogen J., Wan J., Mayes M. A., Keiser A. D., Mo L., ... Maynard D. S. (2019).
497 The global soil community and its influence on biogeochemistry. *Science*, 365(6455).
498 <https://doi.org/10.1126/science.aav0550>.
- 499 Dirmeyer P. A., Gao X., Zhao M., Guo Z., Oki T. & Hanasaki N. (2006). GSWP-2: Multimodel Analysis
500 and Implications for Our Perception of the Land Surface. *Bulletin of the American Meteorological*
501 *Society*, 87(10), 1381–1398. <https://doi.org/10.1175/BAMS-87-10-1381>.
- 502 Georgiou K., Abramoff R. Z., Harte J., Riley W. J. & Torn M. S. (2017). Microbial community-level
503 regulation explains soil carbon responses to long-term litter manipulations. *Nature communications*,
504 8(1), 1223. <https://doi.org/10.1038/s41467-017-01116-z>.
- 505 German D. P., Marcelo K. R. B., Stone M. M. & Allison S. D. (2012). The Michaelis-Menten kinetics of
506 soil extracellular enzymes in response to temperature: a cross-latitudinal study. *Global change*
507 *biology*, 18(4), 1468–1479.
- 508 Geyer K. M., Kyker-Snowman E., Grandy A. S. & Frey S. D. (2016). Microbial carbon use efficiency:
509 accounting for population, community, and ecosystem-scale controls over the fate of metabolized
510 organic matter. *Biogeochemistry*, 127(2), 173–188. <https://doi.org/10.1007/s10533-016-0191-y>.
- 511 Guenther A. B., Jiang X., Heald C. L., Sakulyanontvittaya T., Duhl T., Emmons L. K. & Wang X. (2012).
512 The Model of Emissions of Gases and Aerosols from Nature version 2.1 (MEGAN2.1): an extended
513 and updated framework for modeling biogenic emissions. *Geoscientific Model Development*, 5(6),
514 1471–1492.
- 515 Hashimoto S., Carvalhais N., Ito A., Migliavacca M., Nishina K. & Reichstein M. (2015). Global
516 spatiotemporal distribution of soil respiration modeled using a global database. *Biogeosciences*, 12,
517 4121–4132.
- 518 Jian J., Steele M. K., Day S. D. & Thomas R. Q. (2018a). Future global soil respiration rates will swell
519 despite regional decreases in temperature sensitivity caused by rising temperature. *Earth's Future*, 6
520 (11), 1539-1554.
- 521 Jian J., Steele M. K., Thomas R. Q., Day S. D. & Hodges S. C. (2018b). Constraining estimates of global
522 soil respiration by quantifying sources of variability. *Global change biology*.

- 523 <https://doi.org/10.1111/gcb.14301>.
- 524 Jian J., Vargas R., Anderson-Teixeira K., Stell E., Herrmann V., Horn M., ... Bond-Lamberty B. (2020).
525 A restructured and updated global soil respiration database (SRDB-V5). *Earth System Science Data*
526 *Discussions*, 1–19.
- 527 Jung M., Schwalm C., Migliavacca M., Walther S., Camps-Valls G., Koirala S., ... Walker A. (2019).
528 Scaling carbon fluxes from eddy covariance sites to globe: Synthesis and evaluation of the
529 FLUXCOM approach. *Biogeosciences discussions* , 1–40. <https://doi.org/10.5194/bg-2019-368>.
- 530 Konings A. G., Bloom A. A., Liu J., Parazoo N. C., Schimel D. S. & Bowman K. W. (2019). Global
531 satellite-driven estimates of heterotrophic respiration. *Biogeosciences* , 16(11), 2269–2284.
532 <https://doi.org/10.5194/bg-16-2269-2019>.
- 533 Koven C. D., Hugelius G., Lawrence D. M. & Wieder W. R. (2017). Higher climatological temperature
534 sensitivity of soil carbon in cold than warm climates. *Nature climate change*, 7(11), 817–822.
535 <https://doi.org/10.1038/nclimate3421>.
- 536 Lawrence D. M., Fisher R. A., Koven C. D., Oleson K. W., Swenson S. C., Bonan G., ... Zeng X. (2019).
537 The Community Land Model Version 5: Description of New Features, Benchmarking, and Impact of
538 Forcing Uncertainty. *Journal of Advances in Modeling Earth Systems*, 11(12), 4245–4287.
539 <https://doi.org/10.1029/2018MS001583>.
- 540 Oleson K. W., Lawrence D. M., Bonan G. B. & Flanner M. G. (2010). Technical description of version
541 4.5 of the Community Land Model (CLM), NCAR Tech. Notes (NCAR/TN-478+ STR).
- 542 Potter C. S., Randerson J. T., Field C. B., Matson P. A., Vitousek P. M., Mooney H. A. & Klooster S. A.
543 (1993). Terrestrial ecosystem production: A process model based on global satellite and surface data.
544 *Global biogeochemical cycles*, 7(4), 811–841. <https://doi.org/10.1029/93GB02725>.
- 545 Randerson J. T. & Thompson M. V. (1996). Substrate limitations for heterotrophs: Implications for
546 models that estimate the seasonal cycle of atmospheric CO₂. *Global*.
- 547 Schmidt M. W. I., Torn M. S., Abiven S., Dittmar T., Guggenberger G., Janssens I. A., ... Trumbore S. E.
548 (2011). Persistence of soil organic matter as an ecosystem property. *Nature*, 478(7367), 49–56.
549 <https://doi.org/10.1038/nature10386>.
- 550 Shao P., Zeng X., Moore D. J. P. & Zeng X. (2013). Soil microbial respiration from observations and
551 Earth System Models. *Environmental research letters: ERL [Web site]*, 8(3), 034034.
552 <https://doi.org/10.1088/1748-9326/8/3/034034>.
- 553 Shi Z., Allison S. D., He Y., Levine P. A., Hoyt A. M., Beem-Miller J., ... Randerson J. T. (2020). The

554 age distribution of global soil carbon inferred from radiocarbon measurements. *Nature geoscience*,
555 13(8), 555–559. <https://doi.org/10.1038/s41561-020-0596-z>.

556 Stocker T. F., Qin D., Plattner G.-K., Tignor M., Allen S. K., Boschung J., ... Wuebbles, D. (2013).
557 Climate change 2013: The physical science basis. *Contribution of working group I to the fifth*
558 *assessment report of the intergovernmental panel on climate change*, 1535.

559 Sulman B. N., Moore J. A. M., Abramoff R., Averill C., Kivlin S., Georgiou K., ... Classen A. T. (2018).
560 Multiple models and experiments underscore large uncertainty in soil carbon dynamics.
561 *Biogeochemistry*, 141(2), 109–123. <https://doi.org/10.1007/s10533-018-0509-z>.

562 Sulman B. N., Phillips R. P., Oishi A. C., Shevliakova E. & Pacala S. W. (2014). Microbe-driven
563 turnover offsets mineral-mediated storage of soil carbon under elevated CO₂. *Nature climate change*,
564 4(12), 1099–1102.

565 Sulman B. N., Brzostek E. R., Medici C., Shevliakova E., Menge D. N. L. & Phillips R. P. (2017).
566 Feedbacks between plant N demand and rhizosphere priming depend on type of mycorrhizal
567 association (ed Cleland E.). *Ecology letters*, 20(8), 1043–1053. <https://doi.org/10.1111/ele.12802>.

568 Tang X., Fan S., Du M., Zhang W., Gao S., Liu S., ... Yang W. (2020). Spatial-and temporal-pattern of
569 global soil heterotrophic respiration in terrestrial ecosystems. *earth-syst-sci-data-discuss.net*, 12(2),
570 1037–1051. <https://doi.org/10.5194/essd-12-1037-2020>.

571 Tan Z., Leung L. R., Li H.-Y., Tesfa T., Zhu Q. & Huang M. (2020). A substantial role of soil erosion in
572 the land carbon sink and its future changes. *Global change biology*.
573 <https://doi.org/10.1111/gcb.14982>.

574 Todd-Brown K. E., Randerson J. T. & Post W. M. (2013). Causes of variation in soil carbon simulations
575 from CMIP5 Earth system models and comparison with observations. *Biogeosciences*.

576 Todd-Brown K. E. O., Hopkins F. M., Kivlin S. N. & Talbot J. M. (2012). A framework for representing
577 microbial decomposition in coupled climate models. *Biogeochemistry*.

578 Tramontana G., Jung M., Schwalm C. R., Ichii K., Camps-Valls G., Ráduly B., ... Papale D. (2016).
579 Predicting carbon dioxide and energy fluxes across global FLUXNET sites with regression
580 algorithms. *Biogeosciences*, 13(14), 4291–4313.

581 Wang Y. P., Law R. M. & Pak B. (2010). A global model of carbon, nitrogen and phosphorus cycles for
582 the terrestrial biosphere. *Biogeosciences*, 7(7).

583 Warner D. L., Bond-Lamberty B., Jian J., Stell E. & Vargas R. (2019). Spatial predictions and associated
584 uncertainty of annual soil respiration at the global scale. *Global biogeochemical cycles*, 7, 983.

585 <https://doi.org/10.1029/2019GB006264>.

586 Werf G. R. van der, van der Werf G. R., Randerson J. T., Giglio L., van Leeuwen T. T., Chen Y., ...
587 Kasibhatla P. S. (2017). Global fire emissions estimates during 1997–2016. *Earth System Science*
588 *Data*, 9(2), 697–720.

589 Wieder W. R., Bonan G. B. & Allison S. D. (2013). Global soil carbon projections are improved by
590 modelling microbial processes. *Nature climate change*, 3(10), 909–912.
591 <https://doi.org/10.1038/nclimate1951>.

592 Wieder W. R., Grandy A. S., Kallenbach C. M. & Bonan G. B. (2014). Integrating microbial physiology
593 and physio-chemical principles in soils with the Microbial-MIneral Carbon Stabilization (MIMICS)
594 model. *Biogeosciences*, 11(14), 3899.

595 Wieder W. R., Grandy A. S., Kallenbach C. M., Taylor P. G. & Bonan G. B. (2015a). Representing life in
596 the Earth system with soil microbial functional traits in the MIMICS model. *Geoscientific Model*
597 *Development Discussions*, 8(2).

598 Wieder W. R., Hartman M. D., Sulman B. N., Wang Y.-P., Koven C. D. & Bonan G. B. (2018). Carbon
599 cycle confidence and uncertainty: Exploring variation among soil biogeochemical models. *Global*
600 *change biology*, 24(4), 1563–1579. <https://doi.org/10.1111/gcb.13979>.

601 Wieder W. R., Sulman B. N., Hartman M. D., Koven C. D. & Bradford M. A. (2019). Arctic Soil
602 Governs Whether Climate Change Drives Global Losses or Gains in Soil Carbon. *Geophysical*
603 *research letters*, 46(24), 14486–14495. <https://doi.org/10.1029/2019GL085543>.

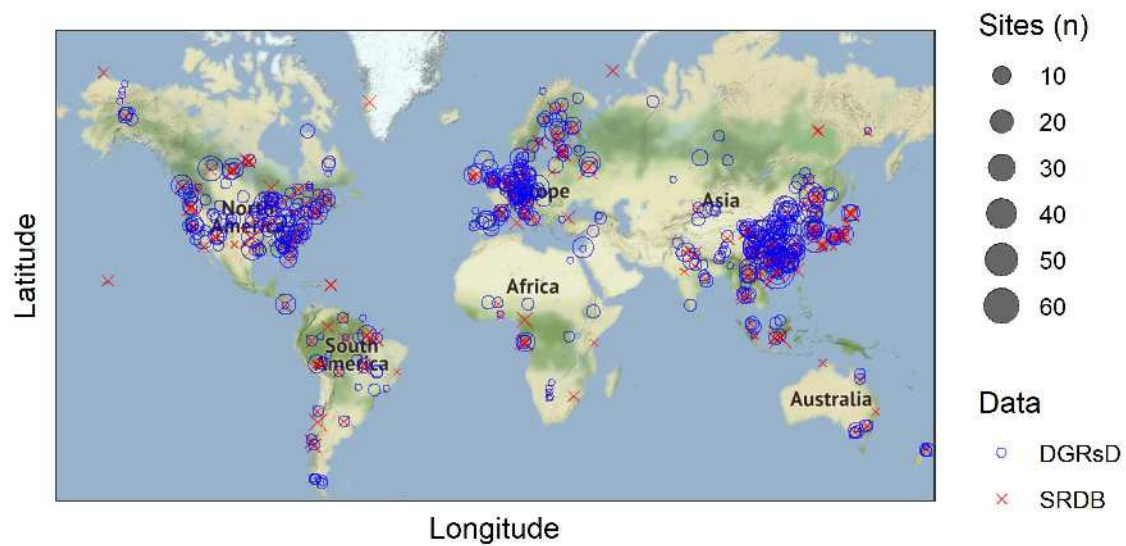
604 Wieder W. R., Allison S. D., Davidson E. A., Georgiou K., Hararuk O., He Y., ... Xu X (2015b).
605 Explicitly representing soil microbial processes in Earth system models. *Global biogeochemical*
606 *cycles*, 29(10), 1782–1800.

607 Yang J. M., Yang J. Y., Liu S. & Hoogenboom G. (2014). An evaluation of the statistical methods for
608 testing the performance of crop models with observed data. *Agricultural systems*, 127, 81–89.
609 <https://doi.org/10.1016/j.agsy.2014.01.008>.

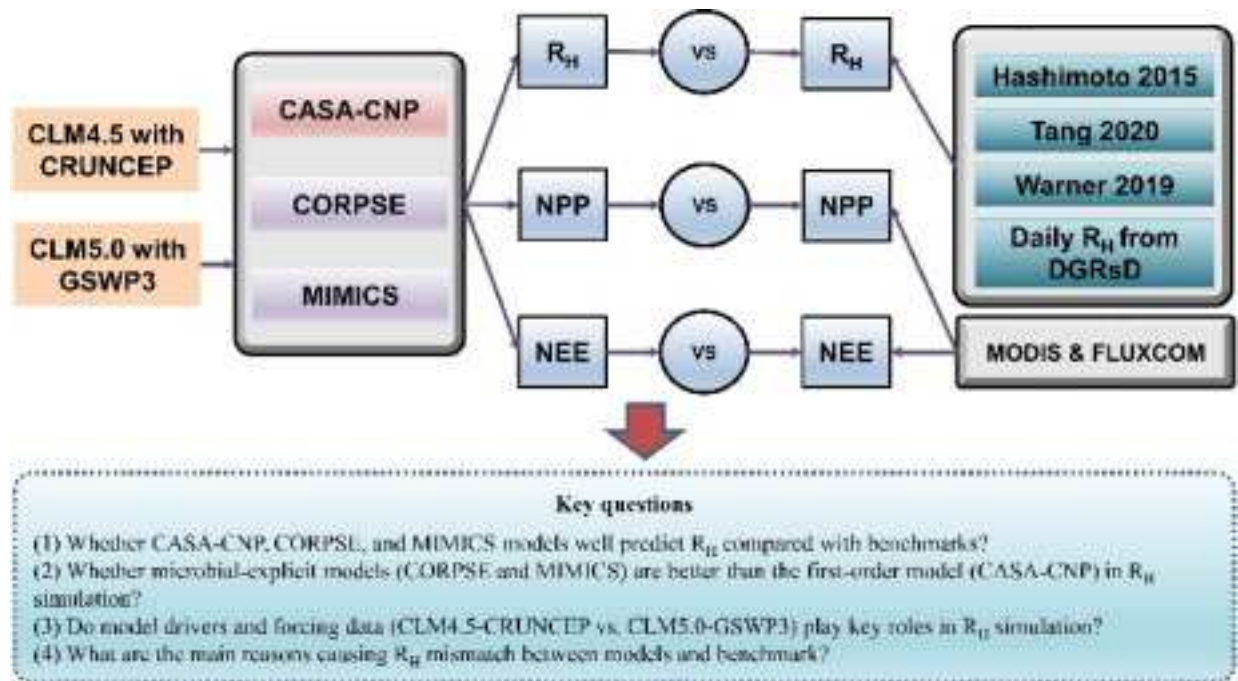
610 Yoshimura K. & Kanamitsu M. (2013). Incremental Correction for the Dynamical Downscaling of
611 Ensemble Mean Atmospheric Fields. *Monthly Weather Review*, 141(9), 3087–3101.
612 <https://doi.org/10.1175/MWR-D-12-00271.1>.

613 Zhang H., Goll D. S., Wang Y.-P., Ciais P., Wieder W. R., Abramoff R., ... Tang X. (2020). Microbial
614 dynamics and soil physicochemical properties explain large-scale variations in soil organic carbon.
615 *Global change biology*, 26(4).

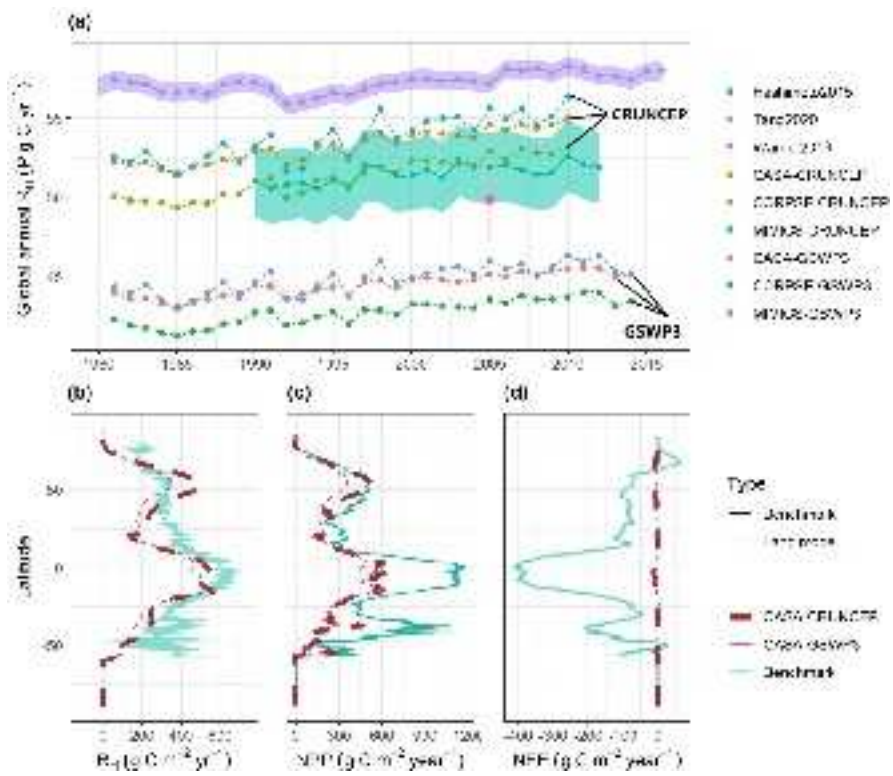
616 Zhao M., Heinsch F. A., Nemani R. R. & Running S. W. (2005). Improvements of the MODIS terrestrial
617 gross and net primary production global data set. *Remote sensing of environment*, 95(2), 164–176.
618 <https://doi.org/10.1016/j.rse.2004.12.011>.



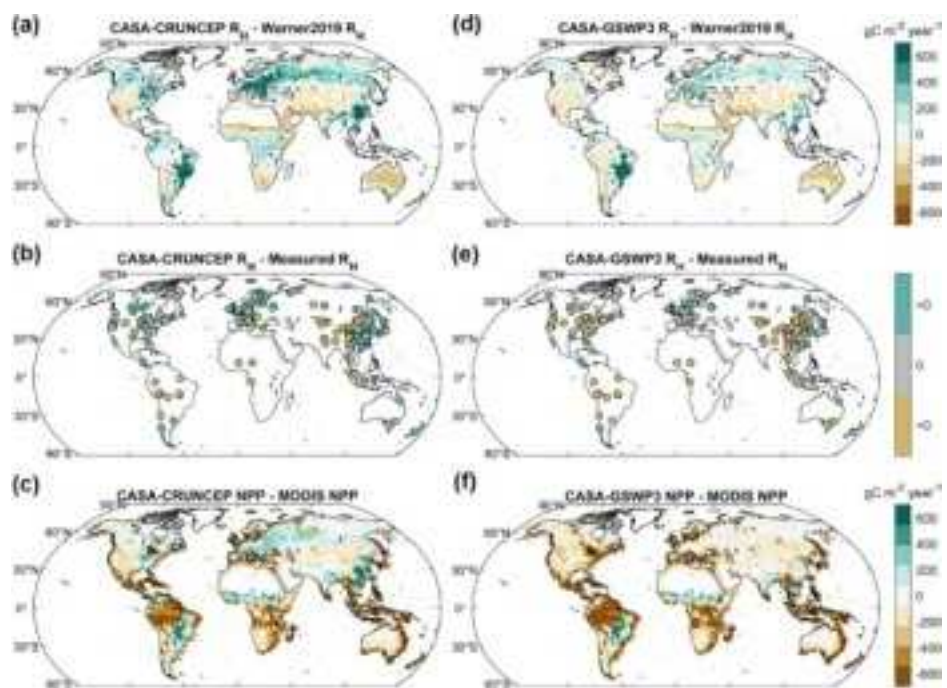
gcb_15795_f1.jpg



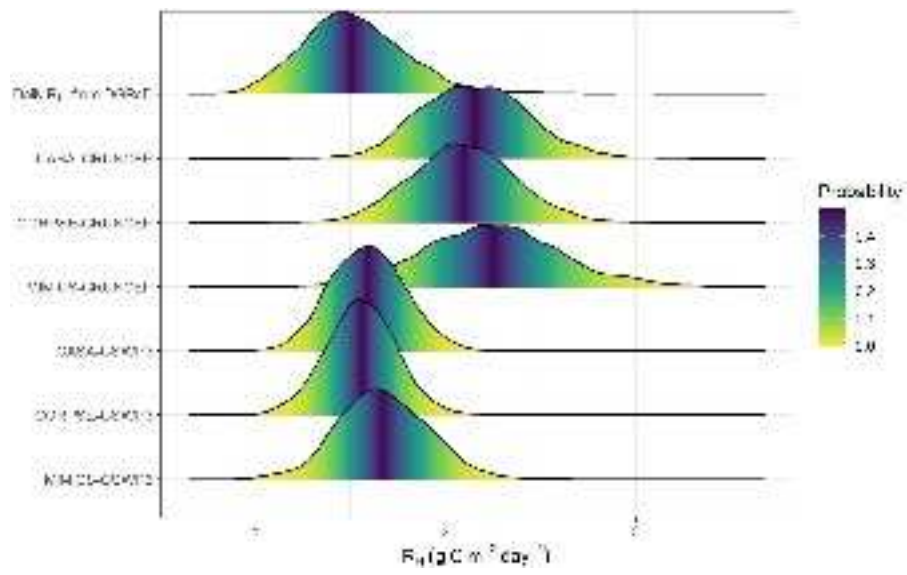
gcb_15795_f2.jpg



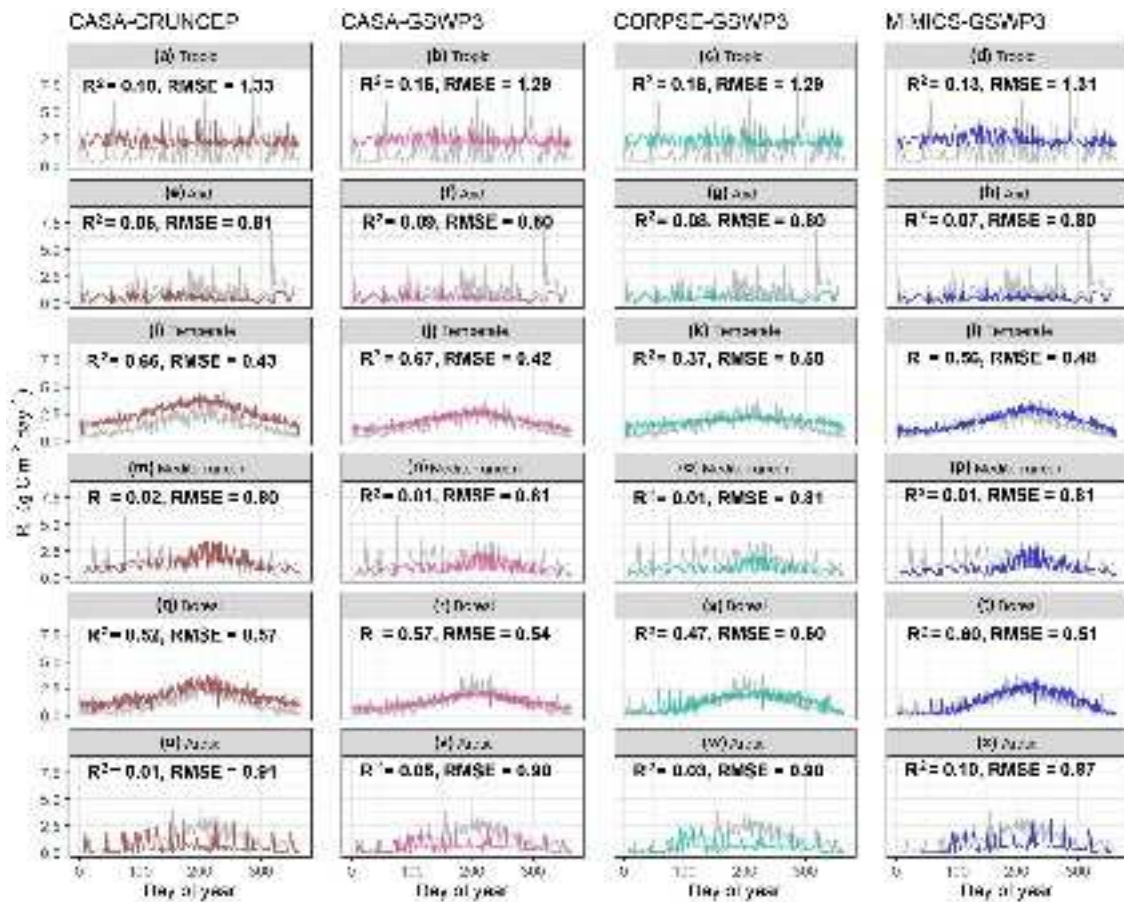
gcb_15795_f3.jpg



gcb_15795_f4.jpg



gcb_15795_f5.jpg



gcb_15795_f6.jpg